International Journal of Fluid Mechanics Research, Vol. 29, No. 6, 2002

Effects of Magnetic Field and Heat Generation/Absorption on Natural Convection from an Isothermal Surface in a Stratified Environment[†]

A. J. Chamkha
Department of Mechanical Engineering, Kuwait University
P. O. Box 5969, Safat, 13060, Kuwait

The problem of steady, laminar, buoyancy-induced flow by natural convection along a vertical permeable surface immersed in a thermally-stratified environment in the presence of magnetic field and heat generation or absorption effects is studied numerically. Conditions for similarity solutions are determined for arbitrary stable and unstable thermal environment stratification. Numerical solution of the resulting similarity equations is performed using an implicit, iterative, tridiagonal finite-difference method. Comparisons with previously published work are performed and the results are found to be in excellent agreement. The effects of the Hartmann number, heat generation or absorption coefficient, ambient temperature power index, and the wall mass transfer parameter on the velocity and temperature profiles as well as the skin-friction coefficient and Nusselt number are presented in graphical form. It is found that both the magnetic field and heat absorption effects eliminate the occurrence of the fluid backflow and temperature deficit in the outer part of the boundary layer predicted for the non-magnetic case.

* * *

Nomenclature

B	magnetic induction;
c_p	specific heat;
C_f	skin-friction coefficient defined by Eq. (13a);
$f(\eta)$	similarity stream function;
g	gravitational acceleration;
$f_0 = \dfrac{v_w}{(-1)^m \dfrac{m+3}{4} 64\,\mathrm{g}\,\beta K N \nu^2}$	dimensionless wall mass transfer parameter;
$\mathrm{Ha}^2 = \dfrac{2\,\sigma B_0^2}{\rho\,(N\,\mathrm{g}\,K\beta)^{1/2}}$	square of the Hartmann number;

[†] Received 18.09.2002.

ISSN 1064-2277
© 2002 Begell House, Inc.

k	thermal conductivity;
K^*	grid growth factor;
K	stratification parameter used in Eq. (5);
m	stratification parameter used in Eq. (5);
M	stratification coefficient used in Eq. (5);
N	stratification coefficient used in Eq. (5);
Nu	Nusselt number defined by Eq. (13b);
Pr	Prandtl number;
Q	heat generation or absorption coefficient;
T	temperature;
u	vertical velocity component;
v	velocity component perpendicular to the plate;
v_w	wall mass transfer parameter;
x	vertical coordinate;
y	coordinate perpendicular to, and beginning at, the plate

Greek symbols

β	coefficient of thermal expansion;
$\delta = \dfrac{Q_0}{\rho c_p N}$	dimensionless internal heat generation/absorption coefficient;
η	similarity y-coordinate;
$\Delta\eta$	gridsize in the η-direction;
μ	dynamic viscosity;
ν	kinematic viscosity;
ρ	density;
σ	electrical conductivity;
θ	similarity temperature;
ψ	stream function;

Superscript

$'$	differentiation with respect to η

Subscripts

w	wall condition;
∞	environment condition.

Introduction

Natural convection flows of electrically-conducting and/or heat-generating or absorbing fluids in the presence of a transverse magnetic field have received considerable interest in recent years. This stems from various industrial and engineering applications involving such flows. Examples of these applications include crystal growth, geothermal systems, heat exchangers, nuclear reactors, metallurgical processes and others. In natural and some industrial free convection heat transfer processes, the density of the fluid is often stably stratified due to the presence of some dissolved species. In most practical situations, the concentration of these species is considered to be dilute. The condition of stable thermal stratification is realized when the fluid temperature increases with height in a gravitational field with the exception of water between $0^\circ\mathrm{C}$ and $4^\circ\mathrm{C}$ as mentioned by

Angirasa and Srinivasan [1].

Analysis and understanding the flow and heat transfer characteristics of processes involving thermal ambient stratification in the presence of heat generation or absorption and magnetic field effects requires the solution of the Navier – Stokes equations. With the use of special transformations, the boundary-layer form of these equations can reduce to a set of ordinary equations (similarity equations) which can be solved numerically with minimum effort. The search for similarity equations started long time ago and has continued in recent years. Ostrach [2] reported an analysis of laminar free convection flow and heat transfer about an isothermal flat plate based on the numerical solution of similarity equations. Sparrow and Gregg [3] reported similar solutions for free convection from a non-isothermal vertical plate. Cheesewright [4] and Yang et al. [5] considered natural convection flow from isothermal and non-isothermal plates immersed in a thermally-stratified environment. Semenov [6] developed similarity solutions for all possible distributions of wall and environment temperatures. Merkin [7] found that a singular behavior is predicted for the case of non-isothermal surface with fixed environment temperature when a critical value of the wall temperature parameter is exceeded. Kulkarni et al. [8] claimed to have found a new class of similarity solutions for natural convection flow over an isothermal vertical wall in a thermally-stratified medium. Later, Henkes and Hoogendoorn [9] reported a general new class of similar solutions for laminar natural convection boundary-layer flow along a heated vertical plate in a stratified environment. Some other related works on thermal stratification can be found in the papers by Chen and Eichhorn [10], Venkatachala and Nath [11], Angirasa and Srinivasan [12] and Angirasa and Peterson [13].

The objective of this work is to consider steady, laminar, natural convection flow along an isothermal vertical permeable surface immersed in a thermally-stratified environment in the presence of a transverse magnetic field, heat generation or absorption and surface mass transfer. The conditions for self-similar solutions are to determined on the basis of the transformations reported earlier by Kulkarni et al. [8].

1. Governing Equations

Consider steady, laminar, natural convection boundary-layer flow along a permeable isothermal vertical surface in a stratified environment in the presence of a transverse magnetic field and internal heat generation or absorption. Both the magnetic field and the internal heat generation/absorption are assumed to vary with the distance along the surface. The fluid properties are assumed to be constant except for the density in the thermal buoyancy term of the governing equations. The magnetic Reynolds number is assumed to be small so that the induced magnetic field can be neglected. This assumption uncouples the Navier – Stokes equations from Maxwell's equations (Cramer and Pai [14]). The governing equations for this investigation are based on the boundary-layer form of the balance laws of mass, linear momentum, and energy. Taking into consideration the Boussinesq approximation, these equations can be written as:

$$\frac{\partial u}{\partial x} + \frac{\partial v}{\partial y} = 0, \tag{1}$$

$$u\frac{\partial u}{\partial x} + v\frac{\partial u}{\partial y} = \nu\frac{\partial^2 u}{\partial y^2} + \mathrm{g}\,\beta\left[T - T_\infty\left(x\right)\right] - \frac{\sigma B^2\left(x\right)}{\rho}\,u, \tag{2}$$

$$u\frac{\partial T}{\partial x} + v\frac{\partial T}{\partial y} = \frac{\nu}{\mathrm{Pr}}\frac{\partial^2 T}{\partial y^2} + \frac{Q\left(x\right)}{\rho c_p}\left[T - T_\infty\left(x\right)\right]u, \tag{3}$$

where the various parameters are defined in the Nomenclature section. The last term in Eq. (3) represents the heat generation/absorption effect and is based on the work of Vajravelu and Hadjinicolaou [15].

The boundary conditions for this problem are given by:

$$\begin{aligned} x = 0: &\quad u \text{ and } T \text{ profiles spesified,} \\ y = 0: &\quad u = 0, \quad v = -v_w(x), \quad T = T_w, \\ y \to \infty: &\quad u = 0, \quad T = T_\infty(x), \end{aligned} \tag{4}$$

where $v_w(x)$, T_w, $T_\infty(x)$ are the wall mass transfer, wall temperature (a constant) and the fluid ambient or environment temperature.

Similarity equations for this problem are possible for special distributions of $B(x)$, $Q(x)$, $v_w(x)$ and $T_\infty(x)$. Kulkarni et al. [8] have proposed the following forms for $T_\infty(x)$, η and $\psi(\eta)$:

$$\begin{aligned} T_\infty(x) &= T_w - K\left[mM + (-1)^m Nx\right]^m, \\ \eta &= \left(\frac{\mathrm{g}\,\beta NK}{4\nu^2}\right)^{1/4} y\left[mM + (-1)^m Nx\right]^{(m-1)/4}, \\ \psi &= \left(\frac{64\,\mathrm{g}\,\beta K}{N^3\nu^2}\right)^{1/4} \nu\left[mM + (-1)^m Nx\right]^{(m+3)/4} f(\eta), \\ \theta &= \frac{T - T_\infty}{T_w - T_\infty}, \end{aligned} \tag{5}$$

where the parameters m, K, M and N are constants that can be determined when the ambient temperature distribution is prescribed.

Defining the stream function in the usual way as

$$u = \frac{\partial \psi}{\partial y}, \qquad v = -\frac{\partial \psi}{\partial x} \tag{6}$$

gives

$$\begin{aligned} u(x,y) &= 2\left(\frac{\mathrm{g}\,\beta K}{N}\right)^{1/2}\left[mM + (-1)^m Nx\right]^{(m+1)/2} f'(\eta), \\ v(x,y) &= -(-1)^m\left(64\,\mathrm{g}\,\beta K N\nu^2\right)^{1/4}\left(\frac{m+3}{4}\right)\left[mM + (-1)^m Nx\right]^{(m-1)/4} f(\eta) \\ &\quad -(4\,\mathrm{g}\,\beta K N)^{1/2}\, y\left(\frac{m-1}{4}\right)(-1)^m\left[mM + (-1)^m Nx\right]^{(m-1)/2} f'(\eta), \end{aligned} \tag{7}$$

where a prime denotes ordinary differentiation with respect to η.

Substitution of Eqs (5)–(7) into Eqs (1)–(4) and assuming that

$$\begin{aligned} B(x) &= B_0\left[mM + (-1)^m Nx\right]^{(m-1)/4}, \\ Q(x) &= Q_0\left[mM + (-1)^m Nx\right]^{-1}, \\ v_w(x) &= \left[mM + (-1)^m Bx\right]^{(m-1)/4}, \end{aligned}$$

(where B_0 and Q_0 are constants) results in the following similarity equations and boundary conditions:

$$f''' + (-1)^m \left[(m+3) f f'' - 2(m+1) f'^2 \right] + \theta - \mathrm{Ha}^2 f' = 0, \tag{8}$$

$$\theta'' + \mathrm{Pr}\,(-1)^m \left[(m+3) f\theta' + 4m(1-\theta) f' \right] + 4\,\mathrm{Pr}\,\delta\,\theta f' = 0, \tag{9}$$

$$\begin{aligned} \eta = 0: \qquad & f = f_0, \qquad f' = 0, \qquad \theta = 1, \\ \eta \to \infty: \qquad & f' \to 0, \qquad \theta \to 0, \end{aligned} \tag{10}$$

where

$$\mathrm{Ha}^2 = \frac{2\sigma B_0^2}{\rho\,(N\,\mathrm{g}\,K\beta)^{1/2}}; \qquad \delta = \frac{Q_0}{\rho c_p N}; \qquad f_0 = \frac{v_w}{(-1)^m \dfrac{m+3}{4} 64\,\mathrm{g}\,\beta K N \nu^2} \tag{11}$$

are the square of the Hartmann number, dimensionless heat generation ($\delta > 0$) or absorption ($\delta < 0$) parameter, and the dimensionless wall mass transfer parameter, respectively. It should be noted that if all of the parameters f_0, Ha and δ are equated to zero, the equations of Kulkarni et al. [8] are recovered.

Eqs (8)–(10) have the property that they contain various special cases. For instance, when m is equated to zero, the model reduces to that of the classical case of T_∞ and T_w where K represents the temperature difference $(T_w - T_\infty)$. When $m = 1$, the ambient temperature increases linearly with x. As mentioned by Kulkarni et al. [8], this is a situation of practical importance for which a similarity solution has not previously been obtained. For this case

$$\eta = \left(\frac{\mathrm{g}\,\beta N K}{4\nu^2} \right)^{1/4} y. \tag{12}$$

For $m = 2, 4, 6, \ldots$ there is unstable stratification and for $m = 3, 5, 7, \ldots$ there is stable stratification. The choice $m = -1$ represents a cold wall in a stably stratified medium and for $m = -2$ the surroundings are either stably stratified or unstably stratified depending on relative values of M and N.

The skin-friction coefficient and the Nusselt number are important physical parameters for this flow and heat transfer situation. They can be defined in dimensionless form as follows:

$$C_f = \xi^{-(1+3n)/4} C_f^* = f''(0), \tag{13a}$$

$$\mathrm{Nu} = \xi^{(1-5n)/4} \mathrm{Nu}^* = -\theta'(0), \tag{13b}$$

where

$$C_f^* = \frac{\mu\,(\partial u/\partial y)_{y=0}}{\mu \left[\left(\mathrm{g}^* \beta \Delta T\right)^3 / \left(\nu^2 |M|\right) \right]^{1/4}} \tag{14}$$

and

$$\mathrm{Nu}^* = \frac{k\,(\partial T/\partial y)_{y=0}}{k \left[\mathrm{g}^* \beta \Delta T^5 |M| / \nu^2 \right]^{1/4}} \tag{15}$$

(μ and k are the fluid dynamic viscosity and thermal conductivity, respectively).

2. Numerical Method

Eqs (8) and (9) are non-linear, coupled, ordinary differential equations which possess no closed-form solution. Therefore, they must be solved numerically subject to the boundary conditions given by Eq. (10). The implicit, iterative finite-difference method discussed by Blottner [16] has proven to be adequate for the solutions of this type of equations. For this reason, this method is employed in the present work.

The method is implemented as follows: first, a change of variable is used in Eq. (8) such that $V = f'$. The resulting equation in V along with Eq. (9) are then expressed in the following general form:

$$\pi_1 F'' + \pi_2 F' + \pi_3 F + \pi_4 = 0, \tag{16}$$

where F is a typical dependent variable which stands for V or θ and the π's are (in general) functions of the dependent and independent variables. At each iteration step, linearization of the equations takes place by evaluating the π's at the previous iteration. Then, all of the equations in the form of Eq. (16) are discretized using three-point central difference quotients. This converts the differential equations into linear sets of algebraic equations which can be readily solved by the well-known Thomas algorithm (see Blottner [16]. With the solution for V known, the equation $f' - V = 0$ is then discretized and solved subject to the appropriate boundary condition by the trapezoidal rule. The computational domain in the η direction was made up of 196 non-uniform grid points. It is expected that most changes in the dependent variables occur in the region close to the surface where viscous effects dominate. However, small changes in the dependent variables are expected far away from the surface. For these reasons, variable step sizes in the η direction are employed. The initial step size $\Delta\eta_1$ and the growth factor K^* employed such that $\Delta\eta_{i+1} = K^* \Delta\eta_i$ (where the subscript i indicates the grid location) were 10^{-3} and 1.03, respectively. These values were found (by performing many numerical experiments) to give accurate and grid-independent solutions. The solution convergence criterion employed in the present work was based on the difference between the values of the dependent variables at the current and the previous iterations. When this difference reached 10^{-5}, the solution was assumed converged and the iteration process was terminated.

3. Results and Discussion

In this section, a representative set of numerical results which illustrates the influence of the Hartmann number Ha, the heat generation or absorption coefficient δ, the mass transfer parameter f_0 and the ambient temperature power index m on the velocity and temperature profiles as well as the skin-friction coefficient and the Nusselt number is shown in Figs 1 – 8.

Figs 1 and 2 present typical velocity and temperature profiles for various values of Ha, f_0 and δ, respectively. The reference curves in these figures correspond to the parametric values in the boxes appearing in these figures. Application of a transverse magnetic field normal to the flow direction gives rise to a resistive force called the magnetic Lorentz force. This force acts in the opposite direction of the flow causing its velocity to decrease and its temperature to increase. In addition, the thermal boundary layer tends to increase as Ha increases. These behaviors are clearly depicted in Figs 1 and 2. In the absence of the magnetic field $(\mathrm{Ha} = 0)$, it was reported by many previous investigators such as Kulkarni et al. [8] and Henkes and Hoogendoorn [9] that a backflow situation is predicted to occur far from the surface while the fluid temperature close to the wall is predicted to be lower than that of the surface. It is clearly seen from Figs 1 and 2 that, for a sufficiently strong magnetic field ($\mathrm{Ha} = 3$), these phenomena do not occur. In general, heat absorption $(\delta < 0)$

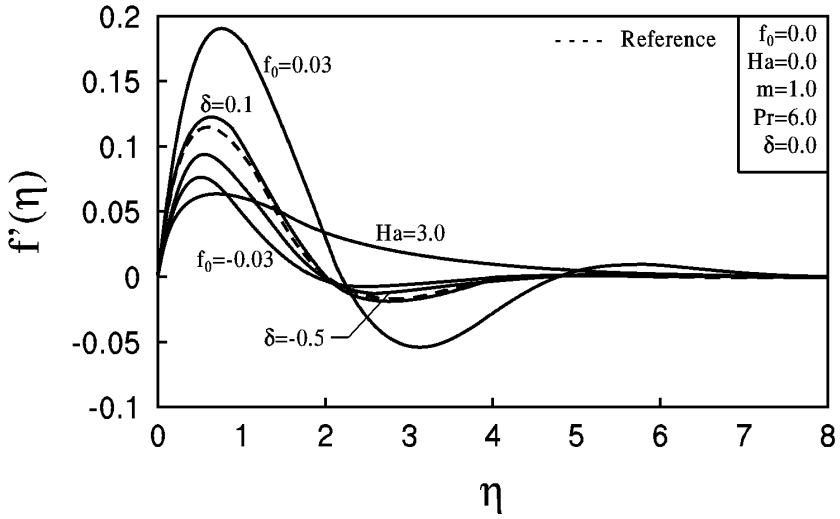

Fig. 1. Typical velocity profiles for various parametric conditions.

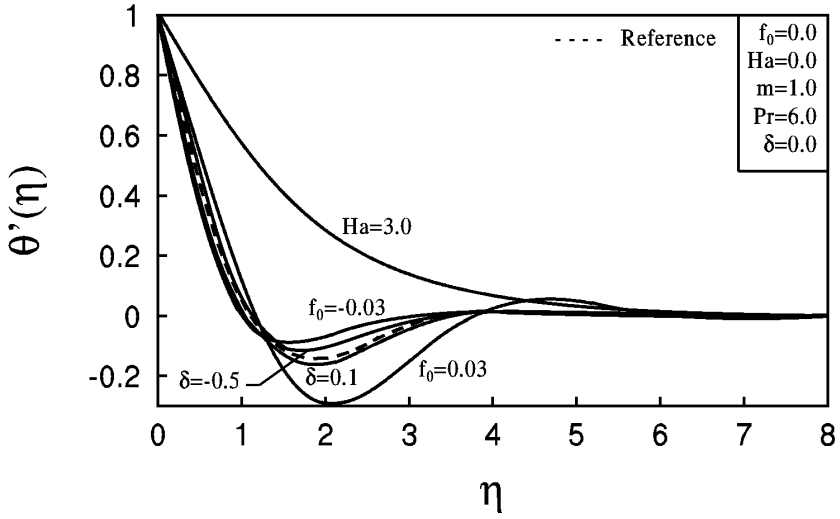

Fig. 2. Typical temperature profiles for various parametric conditions.

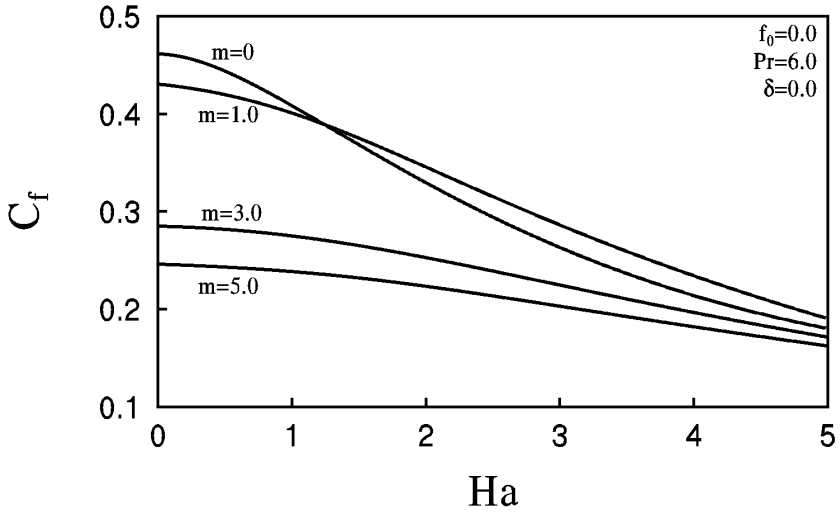

Fig. 3. Effects of Ha and m on the skin-friction coefficient.

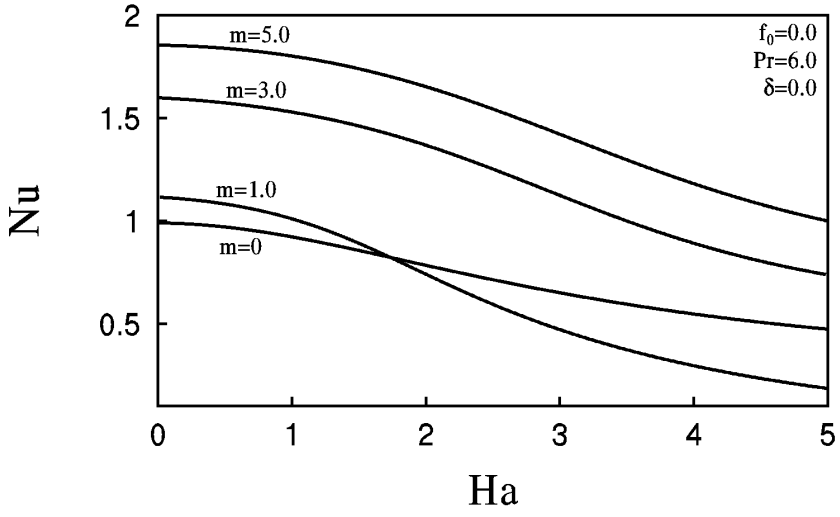

Fig. 4. Effects of Ha and m on the Nusselt number.

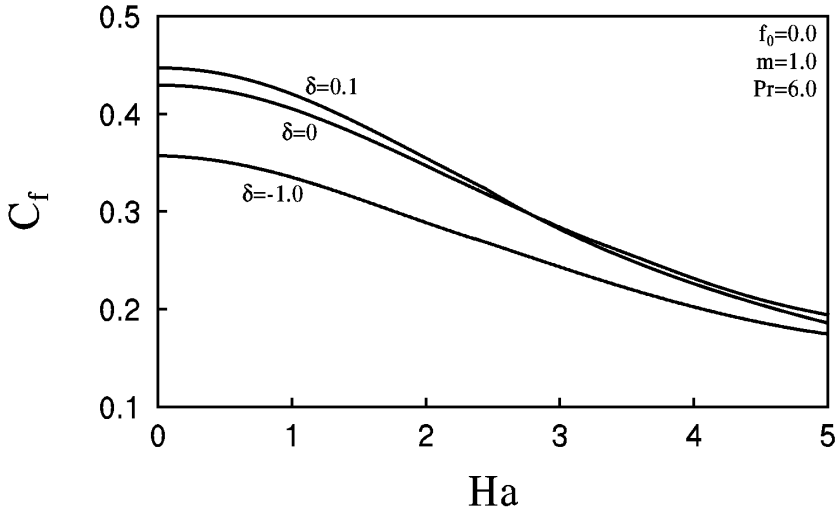

Fig. 5. Effects of Ha and δ on the skin-friction coefficient.

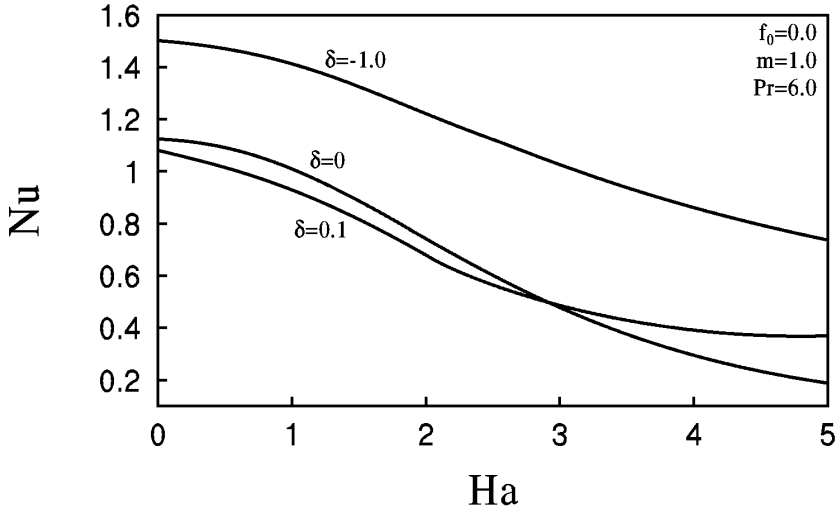

Fig. 6. Effects of Ha and δ on the Nusselt number.

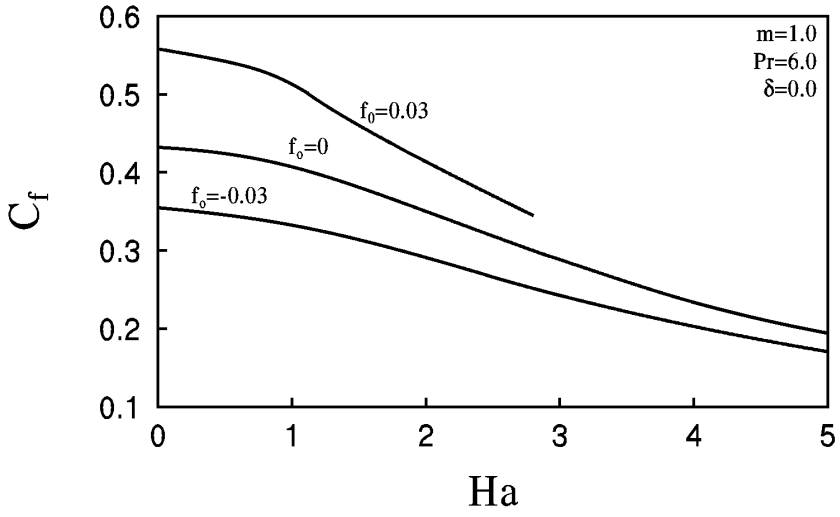

Fig. 7. Effects of Ha and f_0 on the skin-friction coefficient.

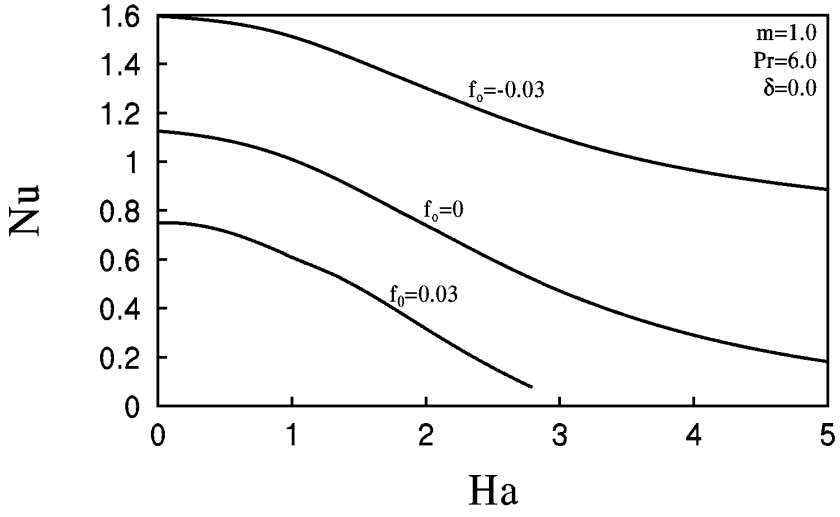

Fig. 8. Effects of Ha and f_0 on the Nusselt number.

has the tendency to reduce the temperature distribution of the fluid along the surface. This causes the buoyancy force to decrease resulting in less flow along the surface. On the other hand, heat generation ($\delta > 0$) enhances the thermal state of the fluid. This has the effect of inducing higher rates of flow along the surface. It is interesting to observe from Figs 1 and 2 that the small backflow and temperature deficit in the outer part of the boundary layer mentioned above can be eliminated by increases in the strength of the heat sink (heat absorption) effect.

Imposition of fluid wall suction ($f_0 < 0$) has the effect of reducing the fluid velocity and increasing its temperature in the region close to the wall. However, in the outer part of the boundary layer, the velocity tends to increase causing the backflow phenomenon there to diminish. In addition, the temperature deficit tends to increase in the outer part of the boundary layer as the suction effect increases. On the other hand, imposition of fluid wall injection ($f_0 > 0$) has the opposite effect on the velocity and temperature profiles, namely, increases in the velocity and reductions in the temperature close to the wall. The backflow condition discussed earlier tends to increase while the temperature deficit diminishes as the injection velocity increases. These behaviors are clearly shown in Figs 1 and 2.

Figs 3 and 4 depict the variations of the skin-friction coefficient C_f and the Nusselt number Nu for various values of Ha and m, respectively. As discussed before, increases in the Hartmann number produce lower velocities along the vertical surface. As a result, the wall slope of the velocity profile decreases. This has the direct effect of decreasing the skin-friction coefficient. This is true for all values of m considered. Similarly, as Ha increases, the wall negative slope of the temperature profile decreases causing the Nusselt number to decrease. These behaviors are depicted by the decreases in C_f and Nu as Ha increases as shown in Figs 3 and 4. Furthermore, it is predicted that as the ambient temperature power index m increases, the skin-friction coefficient decreases while the Nusselt number increases for all values of Ha except for the curves associated with $m = 0$ and $m = 1$ where beyond $\mathrm{Ha} \cong 1.1$, C_f for $m = 1$ is greater than that for $m = 0$. However, beyond $\mathrm{Ha} \cong 1.7$, Nu for $m = 0$ is greater than that for $m = 1$.

Figs 5 and 6 illustrate the influence of Ha and δ on the values of C_f and Nu, respectively. The reductions in the velocity profiles as δ is reduced below zero (heat absorption) discussed earlier cause its wall slope to decrease yielding reductions in the values of C_f for all values of Ha considered. However, for $\delta > 0$, the induced flow increases producing higher wall shear stresses except for values of $\mathrm{Ha} > 2.5$ (for $\delta = 0.1$) where C_f decreases slightly due to the fact that the Lorentz force overcomes the increases in the thermal buoyancy produced by increases in δ. Similarly, the wall negative slope of the temperature profile is increased as δ drops below zero (heat absorption) causing the values of Nu to increase for all values of Ha considered. On the other hand, heat generation produces the opposite effect, namely, a reduction in the values of Nu except for values of $\mathrm{Ha} > 2.9$ (for $\delta = 0.1$) for the same reason as mentioned above. These behaviors are clear from Figs 5 and 6.

Figs 7 and 8 present the effects of f_0 on C_f and Nu for various values of Ha, respectively. It is predicted that imposition of fluid wall suction ($f_0 < 0$) produces lower values of C_f and higher values of Nu for all values of Ha considered. The opposite effect is observed for the case of fluid wall injection where C_f increases while Nu decreases. It should be mentioned that for $f_0 = 0.03$ convergence difficulties were encountered when Ha was set greater than 2.7. This is probably due to the existence of an inflection point in the temperature profile. These behaviors are clear from Figs 7 and 8.

Conclusion

The problem of steady, laminar, natural convection flow along a heated vertical surface in a thermally-stratified environment in the presence of magnetic field, heat generation or absorption, and wall mass transfer effects was considered. The governing equations for this problem were developed, non-dimensionalized and transformed into a similarity form. The distributions of the magnetic field strength, heat absorption, and wall mass transfer necessary for similarity solutions were determined. Numerical solutions of the similarity equations were obtained using an implicit, iterative, tri-diagonal, finite-difference method. A representative set of graphical results was presented and discussed. It was found that, for a fixed wall temperature, application of a transverse magnetic field or inclusion of heat absorption effects eliminated the backflow and temperature deficit in the outer part of the boundary layer inherent in the non-magnetic case. The imposition of wall fluid suction was predicted to eliminate the backflow condition and to reduce the temperature deficit. However, the imposition of fluid wall injection produced the exact opposite behavior. In addition, increasing the magnetic field strength decreased both the skin-friction coefficient and the Nusselt number for all considered stratified environments. While heat absorption produced lower skin-friction coefficients, it increased the Nusselt number. The effect of fluid wall suction was predicted to decrease the skin-friction coefficient and to increase the Nusselt number.

REFERENCES

1. Angirasa, D. and Srinivasan, J., Natural Convection Heat Transfer from an Isothermal Vertical Surface to a Stable Thermally Stratified Fluid, *ASME J. Heat Transfer*, 1992, **114**, pp. 917–923.
2. Ostrach, S., An Analysis of Laminar Free-Convection Flow and Heat Transfer about a Flat Plate Parallel to the Direction of the Generating Body Force, *NACA Report*, No. 1111, 1953.
3. Sparrow, E. M. and Gregg, J. L., Similar Solutions for Free Convection from a Nonisothermal Vertical Plate, *Trans. ASME*, 1958, **80**, pp. 379–386.
4. Cheesewright, R., Natural Convection from a Plane, Vertical Surface in Non-Isothermal Surroundings, *Int. J. Heat Mass Transfer*, 1967, **10**, pp. 1847–1859.
5. Yang, K. T., Novotny, J. L., and Cheng, Y. S., Laminar Free Convection from a Nonisothermal Plate Immersed in a Temperature Stratified Medium, *Int. J. Heat Mass Transfer*, 1972, **15**, pp. 1097–1109.
6. Semenov, V. I., Similar Problems of Steady-State Laminar Free Convection on a Vertical Plate, *Heat Transfer – Sov. Resch*, 1984, **16**, pp. 69–85.
7. Merkin, J. H., A Note on the Similarity Solutions for Free Convection on a Vertical Plate, *J. Engng Math.*, 1985, **19**, pp. 189–201.
8. Kulkarni, A. K., Jacobs, H. R., and Hwang, J. J., Similarity Solution for Natural Convection Flow over an Isothermal Vertical Wall Immersed in Thermally Stratified Medium, *Int. J. Heat Mass Transfer*, 1987, **30**, pp. 691–698.
9. Henkes, R. A. W. M. and Hoogendoorn, C. J., Laminar Natural Convection Boundary-Layer Flow along a Heated Vertical Plate in a Stratified Environment, *Int. J. Heat Mass Transfer*, 1989, **32**, pp. 147–155.
10. Chen, C. C. and Eichhorn, R., Natural Convection from a Vertical Surface to a Thermally Stratified Fluid, *J. Heat Transfer*, 1976, **98**, pp. 446–451.
11. Venkatachala, B. J. and Nath, G., Nonsimilar Laminar Natural Convection in a Thermally Stratified Fluid, *Int. J. Heat Mass Transfer*, 1981, **24**, pp. 1848–1850.
12. Angirasa, D. and Srinavasan, J., Natural Convection Flows due to the Combined Buoyancy of

Heat and Mass Diffusion in a Thermally Stratified Medium, *ASME J. Heat Transfer*, 1989, **111**, pp. 657–663.

13. Angirasa, D. and Peterson, G. P., Natural Convection Heat Transfer from an Isothermal Vertical Surface to a Fluid Saturated Thermally Stratified Porous Medium, *Int. J. Heat Mass Transfer*, 1997, **40**, pp. 4329–4335.
14. Cramer, K. R. and Pai, S.-I., *Magnetofluid Dynaimcs for Engineers and Applied Physicists*, New York, McGraw-Hill Book Company, 1973.
15. Vajravelu, K. and Hadjinicolaou, A., Convective Heat Transfer in an Electrically Conducting Fluid at a Stretching Surface with Uniform Free Stream, *Int. J. Engng. Sci.*, 1997, **35**, pp. 1237–1244.
16. Blottner, F. G., Finite-Difference Methods of Solution of the Boundary-Layer Equations, *AIAA J.*, 1970, **8**, pp. 193–205.

❑◆◆◆❑